LPCVD silicon-rich silicon nitride films for applications in micromechanics, studied with statistical experimental design*

J. G. E. Gardeniers[a] and H. A. C. Tilmans[b]
MESA Research Institute, University of Twente, P.O. Box 217, NL-7500 AE Enschede, The Netherlands

C. C. G. Visser
DIMES, Delft University of Technology, P.O. Box 5053, NL-2600 GB Delft, The Netherlands

(Received 29 March 1996; accepted 28 June 1996)

A systematic investigation of the influence of the process parameters temperature, pressure, total gas flow, and SiH_2Cl_2:NH_3 gas flow ratio on the residual stress, the refractive index, and its nonuniformity across a wafer, the growth rate, the film thickness nonuniformity across a wafer, and the Si/N incorporation ratio of low pressure chemical vapor deposition Si_xN_y films has been performed. As a tool for complete characterization of the property-deposition parameter relations, a full factorial experimental design was used to determine the dominant process parameters and their interactions. From this study it could be concluded that, in decreasing order of importance, the gas flow ratio of Si and N containing precursors, temperature, and pressure are the most relevant parameters determining the mechanical and optical properties of the films and the deposition rate and nonuniformity in film properties across a wafer. The established relations between properties and deposition parameters were fitted with physical–chemical models, including a film growth model based on a Freundlich adsorption isotherm. The optimal deposition conditions for films to be used in micromechanical devices will be discussed. © *1996 American Vacuum Society*.

I. INTRODUCTION

Thin films of silicon nitride, Si_xN_y, are of special interest for microsystem technology, e.g., as a construction material in micromechanical sensors[1] or in x-ray masks.[2] One of the commonly used processes in this field is low pressure chemical vapor deposition (LPCVD) of the material from a gas mixture of dichlorosilane (DCS), SiH_2Cl_2, and ammonia, NH_3, at temperatures between 700 and 900 °C, the use of low pressures (below 1 Torr) generally results in an excellent uniformity of film thickness and composition and conformal step coverage.[3] Standard processes as used in the integrated circuit (IC) industry, where silicon nitride is used as a passivation layer or as a mask for the selective oxidation of silicon, employ an excess of ammonia, resulting in a nearly stoichiometric Si_3N_4 film. Because of the large tensile residual stress existing in these films, they are less suitable as a construction material in mechanical devices, like resonant strain gauge sensors.[1] As was shown by Sekimoto *et al.*,[2] stress reduction and even stress reversal from tension to compression can be accomplished when an excess of DCS is used. It seems that the deposition of Si-rich Si_xN_y is more sensitive to variations in processing conditions than that of stoichiometric Si_3N_4. For example, hardly any changes in the refractive index or the film stress occur if the DCS:NH_3 mole ratio is varied from 1:2 to 1:20,[4,5] while in the case of Si-rich films only small changes in the DCS:NH_3 mole ratio can result in relatively large variations in the index and the mechanical stress.[2]

This article describes the results of a systematic investigation of the influence of process parameters in LPCVD of Si-rich Si_xN_y on several properties of the resulting films. The primary parameters that control the growth of thin films in this process are temperature, total pressure, total gas flow, and reactant concentrations (gas flow ratios). The influence of these parameters will be studied with the aid of a statistical factorial experimental design.[6–8] Factorial experiments are very useful for measurement problems in which a large number of experimental parameters are involved; they are especially suited for systems in which interactions between parameters exist, which are not simple superpositions of the individual effects of the parameters. The determination of the relation between film properties and deposition variables in an LPCVD reactor is such a measurement problem. This is the reason why several researchers have applied factorial designs to investigate electrical properties[9] and thickness uniformity[10] of LPCVD Si_xN_y films as a function of deposition conditions. In our study a full factorial design[6] will be used as a tool for process characterization. The results will be interpreted on the basis of theoretical (or empirical, if no adequate theory is available) models.

II. EXPERIMENTAL PROCEDURE

A. LPCVD equipment and processes

Most of the experimental work was performed in a commercially available LPCVD hot-wall reactor (ASM) equipped with a 135/141 mm quartz tube. The three-zone reactor was resistance-heated and the evacuation system consisted of a Leybold–Heraeus two-stage mechanical rotary pump (65 m^3/h). The process was microprocessor controlled. The gas flow rate was controlled by mass flow controllers,

*Published without author corrections.

[a]Author to whom correspondence should be addressed; Electronic mail: gds@el.utwente.nl
[b]Present address: CP Clare Corporation, Overhaamlaan 40, B-3700 Tongeren, Belgium.

TABLE I. Responses and measurement techniques.

Response	Measurement technique
Residual stress (σ_0)[a]	Wafer curvature, modified bulge method
Refractive index (n)[a]	Ellipsometry (632.8 nm)
Refractive index nonuniformity across wafer ($\Delta n/n$)[a]	Ellipsometry
Thickness nonuniformity across wafer ($\Delta d/d$)[a]	Ellipsometry
Deposition rate (R_{dep})	Ellipsometry, deposition time
Atomic ratio of silicon and nitrogen (Si/N)	RBS and AES

[a]The ellipsometric data (thickness and refractive index) were obtained by averaging over nine points arranged in a 3×3 matrix; the nonuniformities in thickness and refractive index are the standard deviations for these average values.

while the process pressure was measured at the gas inlet by a Baratron gauge (0–10 Torr). Pressure control was accomplished by injection of nitrogen at the pump inlet. Temperature profiling of the reactor tube was done under vacuum conditions in 200 mTorr N_2. A flat temperature profile was set over a length of 20 cm. To check the generality of the results, some experiments were performed in another reactor (Tempress), which had the same configuration, except for a flat temperature zone of 25 cm.

The process scheme for both reactors was practically the same: before the beginning of a run or a number of runs, a pre-deposition run was done, during which proper operation of the system was checked, lines were purged, and the tube and other quartz ware were covered with a fresh layer of Si_xN_y. This procedure improved the reproducibility of the process.

Before the silicon wafers were loaded, they were run through a cleaning cycle consisting of: fuming HNO_3 (5 min), de-ionized H_2O rinse, boiling HNO_3 (10–15 min), and de-ionized H_2O rinse, and dried by spinning. The wafers were manually loaded into the reactor tube and positioned concentric with the tube, with their polished sides facing the inlet side of the system; three dummy wafers were placed in front of and behind the process wafers. The wafer spacing was 6.6 mm for the ASM and 4.5 or 9.0 mm for the Tempress reactor. Substrates used were 2 in. (for the ASM reactor) or 31 in. (100) Si wafers (for the Tempress reactor), phosphorous doped (5–10 Ω cm) and (280±25) μm thick in the case of 2 in., and (380±25) μm in the case of 3 in. wafers.

B. Design of the experiments

A complete experiment, in order to find Si_xN_y films with optimal mechanical properties for micromechanical sensors, would be composed of three phases: I. a screening experiment, II. a response surface experiment, and III. an optimization experiment. Depending on the particular application, simultaneous optimization of parameters other than mechanical (e.g., refractive index for mechano-optical devices) may be desirable. Since in this article we do not intend to focus on one particular application, optimization experiments will not be discussed here, and only the first two phases will be described in detail.

The screening experiment in this study consists of a two-level full factorial experiment,[6–8] aimed at the selection of the relevant primary deposition parameters (to be called ''factors'') with respect to their influence on the film properties (to be called ''responses''). Although two-level factorial designs are unable to explore a wide region of the factor space, they can determine which variables have a statistically significant influence on the output, thus indicating a promising direction for further experimentation.

The second phase of the experiment consists of a ''response surface experiment''[6–8] on the factors that showed the most significant impact on the film properties during the screening phase. The outcome of this experiment will be a relationship between one or more measured responses and a number of factors. From this experiment, a measure can be obtained of the sensitivity of a particular response to factor variations. For our purposes the residual film stress is the most interesting response. One specific goal of the experiment is to find the processing conditions for growing films with very low tensile strain (smaller than 5×10^{-4}). Such films are most suited as the primary construction layer in, e.g., surface-micromachined silicon beam resonators.[1,11]

C. Measurement techniques

The output responses together with the measurement techniques used are listed in Table I. In phase I of the experiment the film stress was determined with the aid of a modified bulge method.[12] In the original bulge method,[13] a known pressure difference is applied across a membrane which is composed of the film material to be investigated. The relationship between pressure and deflection at the center of the diaphragm is measured. The residual stress σ_0 (and in fact also the Young's modulus) can be determined from a curve fit through the measured data points. In the modified bulge method the force of the stylus of a mechanical surface profilometer is used to cause a deflection of the membrane. The deflection versus load curve will obey a relation of the kind[12]

$$F = C_1\sigma_0 d w_0 + C_2\psi(w_0^3) \tag{1}$$

in which d is the film thickness and $\psi(w_0^3)$ is a function of the third power of the deflection of the center of the membrane, w_0; since C_1 and C_2 are constants which are difficult to obtain exactly,[12] the absolute value of σ_0 obtained from

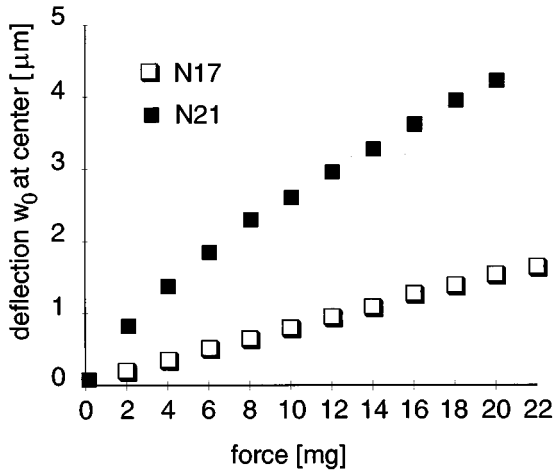

FIG. 1. Deflection w_0 at the center of the diaphragm vs the applied weight, measured on two different samples (see Table III for sample identification codes). The dimension of the diaphragms was 435×435 μm^2.

load-deflection plots with the help of this equation will be incorrect, which is a serious drawback of the method. Measurements of σ_0 on different films can, however, still be compared, if the measurement conditions are kept as constant as possible (e.g., membranes of the same size and shape, and films with approximately the same Young's modulus should be used). Another drawback of the method (and of bulge methods in general) is that it is not possible to measure films that are under compressive stress. For these reasons we have used the bulge method only in the screening experiment to obtain qualitative information on the residual stress. The Si_xN_y membranes required in the modified bulge test were fabricated by etching holes from the backside through the wafers with the aid of a 33 wt % aqueous KOH solution at 75 °C. During etching the nitride film was protected in a specially designed wafer holder. This precaution is not really necessary, since the KOH etchant etches the Si_xN_y layer with a rate of less than 2 nm/h,[11,14] with etch rates almost independent of the Si content of the layer.[14] The width of the resulting square diaphragms was (0.44 ± 0.02) mm. Figure 1 shows some typical load-deflection data. Residual stresses were obtained from the slope of such curves at low deflection, which according to Eq. (1) should be equal to $(C_1\sigma_0 d)^{-1}$. The value of C_1 was estimated from the data in Fig. 3 of Ref. 12, and was found to be 1.6.

The thickness and the refractive index of the silicon nitride films, as well as the nonuniform across the wafer of these two properties, were measured with a Gärtner or a Plasmos ellipsometer, both at a single wavelength of 632.8 nm (see footnote of Table I).

In phase II of the experiment the residual stress was measured by wafer curvature, which allows the determination of both tensile and compressive stresses. The curvature was measured by scanning the surface of the wafers with a mechanical surface profiler (Sloan DEKTAK 3030) in two directions, viz., parallel and perpendicular to the flat. For each wafer three of these measurements were performed: (i) with Si_xN_y ''as-deposited'' on both sides of the wafer, (ii) after removal of the film on the backside, and (iii) after removal of the films on both sides. The differences in curvature between (i) and (ii) and between (ii) and (iii), together with the two different scan directions, give a total of four determinations of residual stress for each wafer. Removal of the Si_xN_y from the backside of the wafer was done by a reactive ion etching process (5 sccm SF_6, 50 sccm N_2, 2.6 W cm^{-2} rf power, at 20 mTorr and 25 °C). During this process the front side of the wafer was protected with a thick photoresist coating. In some cases the curvature of the wafer was too low to be measured accurately. In those cases the wafer was thinned in an aqueous 33 wt % KOH solution at 72 °C (see the remarks above).

Rutherford backscattering (RBS) was used to determine the atomic ratio Si/N of two of the samples of the phase I experiment (samples N17 and N23, see Table III, which will be discussed later). The atomic ratio of the other samples in phase I was obtained from Auger spectroscopy data, using the RBS data as a standard. The film composition was determined from the ratio of the peak-to-peak heights in the $dN(E)/dE$ mode for two combinations of transitions, viz., the Si-*LVV* and N-*KLL* transitions, and the Si-*KLL* and N-*KLL* transitions. According to Keim and Aite,[15] the former of the two ratios is a better probe of the chemical composition.

For a few samples Fourier transform infrared spectroscopy (FTIR) and x-ray diffraction (XRD) were used to determine the hydrogen content (Si–H and N–H bonds) and the crystallinity of the films, respectively.

In this article, we use as a convention that a negative stress value indicates compressive stress.

III. SCREENING EXPERIMENT

As discussed in the foregoing section, the primary deposition parameters for LPCVD Si_xN_y are temperature T, total pressure p, total gas flow ϕ, and the DCS:NH_3 gas flow ratio R. A two-level full factorial experiment on all four factors would require $2^4=16$ runs. In addition, genuine replicate runs are generally required to provide an estimate of the variance or standard deviation of the effects. From literature[2] it is known that temperature is a statistically significant factor. To avoid an excessively large number of runs, the process temperature was not taken as a variable in phase I, but fixed at 800 °C (in the second phase of the experiment temperature will be included, leading to the required information on factor interaction effects).

The experiment performed was a two-level factorial, with pressure, total gas flow, and the gas flow ratio DCS:NH_3 as factors. For a two-level factorial experiment, only factor values at the extremes of their ranges are investigated. To gain some insight into the curvature of factor response, four center point runs are included, in which the factors are set at a value halfway to the extremes of their ranges; replicate center point runs are used to obtain an estimate of the experimental error variance.[6]

TABLE II. Levels for the three factors chosen for study in phase I.

	Levels[a]			
Factor	−	+	0	Unit
Pressure (p)	200	500	350	mTorr
Flow (ϕ)	44	88	66	sccm
Flow ratio (R)[b]	1	10	5	sccm/sccm

[a]The levels are marked ''+,'' ''−,'' and ''0'' for, respectively, the high, low, and center point values. The temperature was fixed at 800 °C.
[b]$R=\phi\ (SiH_2Cl_2)/\phi\ (NH_3)$.

The levels of the factors examined are listed in Table II. From preliminary runs, the deposition rate is approximately known for different processing conditions. The deposition time was chosen such that the film thicknesses were close to 100 nm.

The experimental run design is shown in the first five columns of Table III in the form of a truth table. The high and low values of each variable are represented by a ''+'' and ''−'' symbols, respectively. The center points are indicated by ''0.'' The order of the runs was randomized to reduce bias errors that arise from following a redundant pattern. The actual run order is also listed in Table III.

A. Results

The raw data for phase I, together with the design matrix, are given in Table III. The data were reduced using Yates's algorithm[6] to yield Table IV, which shows the effects of the main factors and their interactions (see Ref. 6 for a general discussion of the meaning of main and interaction effects).

From the RBS measurements it is concluded that the Cl content of the films N23 and N17 is below 1% (see Fig. 2). This is consistent with the results of Gregory *et al.*[9] and Zhang *et al.*,[16] who, with the aid of RBS, found 0.09 and 1 at. % Cl, respectively, in their LPCVD Si_xN_y layers. In our layers the oxygen content was below the detection limit.

B. Conclusions and consequences for the next phase of the experiment

In Table IV the significant effects, i.e., the effects larger than the confidence level S_{95}, have been underlined. From Table IV it can be concluded that for σ_0 and Si/N the mass flow ratio R is the only significant factor (when the temperature is kept constant). As expected, an increase in R results in an increase of the Si/N ratio in the film. Due to the relatively large errors in the determination of the atomic ratios from the RBS and Auger data, the noise level is large. This explains why the DCS/NH_3 ratio shows up as the only significant parameter for this case. Similarly, the large errors in the measurement of stress do not allow the identification of effects other than that of the mass flow ratio.

The refractive index data show a total of four significant effects. For this response R is the most important, while p and the interaction of p and R have a significant influence as well. The effect of total gas flow is marginal; only a significant, slight interaction of ϕ with R is found, which is, how-

TABLE III. Design matrix and raw data of the phase I experiment (ASM reactor, 2 in. wafers).

Wafer id.	Run order	p	ϕ	R	n	σ_0 in MPa	R_{dep} in nm/min	$\Delta d/d$ in %	Si/N[a]	d in nm
N17	3	−	−	−	2.012	830	3.36	0.15	0.77 0.82	100.7
N18	5	+	−	−	1.995	880	4.36	0.58	0.78 0.84	91.6
N19	9	−	+	−	2.015	780	4.66	0.26	0.77 0.83	93.2
N20	1	+	+	−	2.004	880	6.99	0.98	0.78 0.84	90.9
N21	8	−	−	+	2.257	230	1.81	0.61	1.02 0.95	106.8
N22	4	+	−	+	2.353	180	1.92	1.81	1.14 0.98	89.8
N23	10	−	+	+	2.236	250	3.07	0.45	1.04 0.96	104.4
N24	6	+	+	+	2.315	290	3.90	2.28	1.04 0.94	113.2
NC1	7	0	0	0	2.106	660	4.03	0.72	0.87 0.93	121.0
NC2	11	0	0	0	2.092	630	4.02	0.70	0.87 0.97	100.5
NC3	2	0	0	0	2.088	680	4.14	0.78	0.87 0.84	93.2
NC4	12	0	0	0	2.101	660	4.09	0.75	0.87 0.93	112.3

[a]The relative error in the ratios is ~6%; the upper value for each wafer was determined from the Si-LVV:N-KLL peak-to-peak distance ratio, the lower from the Si-KLL:N-KLL ratio (see experimental section).

TABLE IV. Calculated effects for the phase I experiment.[a]

Effect	n	σ_0 (MPa)	R_{dep} (nm/min)	$\Delta d/d$ (%)	Si/N[b]
Mean	2.148	540	3.76	0.89	0.92
					0.90
p	0.037	40	1.07	1.05	0.04
					0.01
ϕ	−0.012	30	1.79	0.21	−0.02
					−0.01
R	0.284	−600	−2.17	0.80	0.29
					0.13
$p\phi$	−0.003	40	0.51	0.23	−0.03
					−0.02
pR	0.051	−40	−0.60	0.47	0.03
					−0.01
ϕR	−0.018	50	−0.17	−0.05	−0.02
					−0.01
$p\phi R$	−0.006	10	−0.15	0.09	−0.03
					−0.01
Mean of NC runs	2.097	660	4.07	0.74	0.87
					0.92
S_1[c]	0.009	30	0.06	0.04	0.05
					0.06
S_{95}[c]	0.014	50	0.09	0.06	0.08
					0.09

[a]The significant effects have been underlined.
[b]See footnote of Table III.
[c]S_1 is an estimate of the standard deviation for a particular response, obtained from either the center point runs, or the measurement accuracy, depending on which of the two is larger; S_{95} is the size of the 95% confidence level for the hypothesis that the effect is due to random fluctuations only; in this particular case $S_{95}=1.6S_1$ (see Ref. 6). Effects are considered statistically significant if they are larger than this 95% level.

ever, very close to S_{95} and therefore not very important.

The deposition rate is a response which includes even a significant three-way interaction. The influence of all three deposition parameters p, ϕ, and R on the deposition rate is strong. Both increases in pressure and flow result in an increased deposition rate. The steepness of the increase in the deposition rate, when either pressure or flow is increased, depends on the levels of the other parameters, as the interaction effects, especially those including the pressure, are also significant. For example, the increase in deposition rate when the pressure is raised from 200 to 500 mTorr is stronger at high flow levels, irrespective of the gas flow ratio. Increasing R, on the other hand, results in a decrease of the deposition rate.

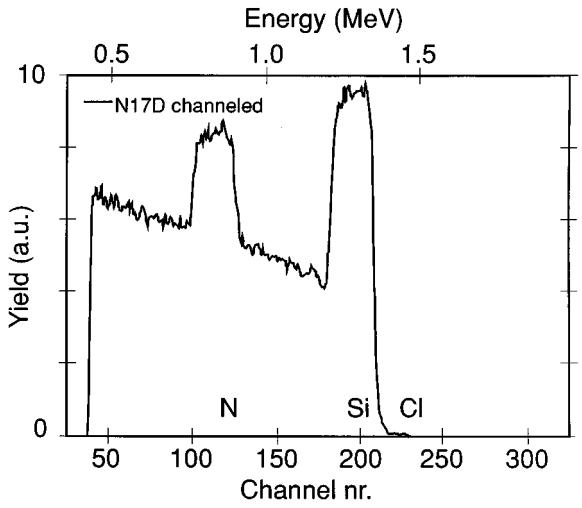

FIG. 2. RBS spectrum of sample N17.

The thickness nonuniformity also shows a complex interaction mechanism among the different deposition variables. Pressure is the most important factor here. As was expected, reduced pressure levels show a better uniformity. But it is also observed that the process of growing stoichiometric nitride (samples N17–N20) yields a better thickness uniformity than the silicon-rich films (samples N21–N24) deposited at higher R values, keeping the other parameters constant.

Some words should be said about the meaning of ''interactions.'' In general, for experimental systems in which the effects of the factors are independent, all interaction effects are found to be zero, which means that the response to a specific change in a certain factor is the same for all values of the other factors, or, in other words, that the response to a combination of changes in several factors is a simple linear superposition of the responses to each individual factor. If one finds nonzero interaction effects in such a case, these effects are due to experimental errors and can thus be used as an estimate of these errors. In fact, in such a situation less experiments are required in order to still obtain sufficient information about the behavior of the experimental system under study. This leads to the development of experimental designs with fractional factorials.[6–8]

However, for most experimental systems (and especially those systems in which a number of complex chemical reactions are running both sequentially as well as parallel, e.g., chemical vapor depositions) the effects of factors are not independent. For those cases, full factorial experiments have to be used to obtain the information required to have a complete picture of the physical–chemical behavior of the system and to be able to construct reliable response surfaces. The significant interaction effects which were found in this study (see Table IV) indicate that for LPCVD of Si_xN_y the choice of a full factorial experiment is a good one.

As mentioned before, it is possible to obtain information about the curvature of the response-factor relation from the center point runs. To investigate this, one should compare the average values of the center point runs with the mean values obtained from the Yates treatment of the measurements; if a linear behavior exists in the factor space between the + and − levels, the Yates values and the mean values should be equal. The mean values are shown in Table IV. Comparison shows that, with the exception of Si/N, all center point runs deviate significantly from the mean values, which suggests a nonlinear response of the investigated film properties to all the important factors.

In conclusion, we have found that the DCS:NH_3 mass flow ratio is the most important factor for most of the studied responses. For several responses, especially those describing the kinetics of the deposition process, viz., R_{dep} and $\Delta d/d$, also the pressure in the reactor tube is important. Statistically significant interactions of these factors have also been found. In the next phase of the experiment we shall therefore have to include both these factors, with an emphasis on the mass flow ratio. The total mass flow ϕ is found to be of less importance; variation of this factor only affects the deposition rate and, to a much lesser extent, the uniformity of deposition. In general, it is preferable to have a high deposition rate, which can best be achieved by an increase in the total gas flow. In the second phase of the experiment, described below, we shall fix the gas flow at the high level of 88 sccm.

TABLE V. Levels for the factors chosen for study in phase II.

Factor	Levels			Unit
	−	+	0	
Pressure (p)	200	410	350	mTorr
Temperature (T)	800	850	−	°C

IV. RESPONSE SURFACE EXPERIMENT

For response surface construction,[6] which, as concluded above, will be done with the factors T, p, and R, at least

TABLE VI. Design matrix and results of the phase II experiment (ASM reactor, 2 in. wafers).

Wafer id.	Run order	T	p	R	n	$\Delta n/n$ in %	σ_0 in MPa[a]	R_{dep} in nm/min	$\Delta d/d$ in %	d in nm
N25A	3	−	−	0.10	1.990	0.08	1300±170	2.57	0.52	51.4
N25	29	−	−	0.10	2.033	0.04	1190± 90	2.86	0.39	100.2
N26	4	−	−	1.00	2.071	0.10	1070±100	5.01	0.19	100.1
N27	5	−	−	5.29	2.204	0.04	680±170	3.68	0.47	92.1
N28	7	−	−	10.0	2.335	0.10	60± 50	3.13	0.72	100.0
N29	6	−	−	13.7	2.548	0.27	40±170	2.66	0.87	98.3
N30	10	−	+	0.10	1.994	0.09	…[b]	3.83	0.70	107.1
N31	9	−	+	1.00	2.031	0.10	1060± 90	6.62	0.84	122.0
N32	11	−	+	5.29	2.252	0.17	…[b]	5.04	1.68	110.8
N33	13	−	+	10.0	2.471	0.33	140± 30	3.60	2.27	89.9
N34	12	−	+	13.7	2.710	0.46	−110± 80	2.90	3.00	69.7
N35	18	+	−	0.10	2.030	0.03	1370±180	4.05	0.77	81.1
N36	15	+	−	1.00	2.065	0.03	960± 90	8.68	0.41	86.8
N37	16	+	−	3.00	2.150	0.06	540±110	7.03	0.69	84.4
N38	17	+	−	5.77	2.304	0.12	110±100	5.35	1.31	74.9
N39	19	+	−	8.78	2.542	0.26	−160±140	4.21	2.02	71.6
N40	25	+	+	0.10	2.024	0.05	1230± 40	4.23	1.31	76.2
N41	23	+	+	1.00	2.064	0.06	1100± 40	10.95	0.96	98.5
N42	27	+	+	3.00	2.173	0.20	660± 40	8.61	1.70	94.8
N43	24	+	+	5.77	2.387	0.41	160±160	5.72	3.31	85.8
N44	26	+	+	8.78	2.717	0.67	0±110	4.12	4.77	65.9
NC10	1	−	0	5.00	2.197	0.11	620± 30	3.64	1.21	91.0
NC11	2	−	0	5.00	2.207	0.11	630± 20	3.84	1.30	95.9
NC12	8	−	0	5.00	2.213	0.10	720±100	4.02	1.26	100.4
NC13	14	−	0	5.00	2.217	0.11	650±110	4.09	1.23	102.2
NC14	21	−	0	5.00	2.215	0.10	…[b]	3.98	1.15	99.4
ND1	20	+	0	5.00	2.299	0.20	250± 50	4.76	2.82	57.1
ND2	22	+	0	5.00	2.327	0.26	220± 90	4.83	2.27	96.7
ND3	28	+	0	5.00	2.338	0.30	170±150	4.88	2.55	97.6

[a]The stresses are the averages obtained from four scans across the wafer, as indicated in the experimental section; the errors are the standard deviations in these averages.
[b]Error in measurement too large (see the text).

three levels for each factor should be used, which allows an approximation of the surface by a quadratic function. A full factorial design thus requires at least $3^3=27$ runs. Although the design requires a large number of runs, it might still not provide a very accurate representation of the functional relationship between factors and responses. Since it was found in phase I of the experiment that the gas flow ratio is the dominating parameter within the range of factor levels examined, we decided to take five levels for this factor, and only two for temperature and pressure.

The variable assignments for this experiment are shown in Tables V and VI. The extreme levels defining the temperature range are based on the results published by Sekimoto *et al.*,[2] who concluded that for the preparation of Si_xN_y films with small residual stress, high temperature deposition is effective. The low level for pressure is the same as during the first phase. Because of the unacceptable nonuniformity levels which we found for depositions at 500 mTorr, the high pressure level is chosen at 410 mTorr. Five levels for the gas flow ratio for every possible combination of pressure and temperature were chosen. The levels for the ratio are not chosen the same for the two different temperatures, because at the high temperature level (850 °C) it is expected that the conditions at which the stress will reach a zero value occur at lower flow ratio levels.[2] In addition to the actual runs, occasionally runs were performed to check possible drift of the system. Two sets, one for every temperature level, were used. The set points for these so-called ''calibration runs'' are: $R=5.00$, $p=350$ mTorr, $\phi=66$ sccm, and $T=800$ °C (''NC'' runs) or $T=850$ °C (''ND'' runs).

Residual film stresses were calculated from wafer curvature measurements with the aid of the following equation (assuming that $t_s \ll d$)[17,18]

$$\sigma_0=\frac{4}{3}\frac{E_s}{(1-\nu_s)}\frac{t_s^2}{d}\frac{\delta}{D^2} \tag{2}$$

in which E_s and ν_s are the Young's modulus and Poisson ratio of the substrate material, respectively (for silicon $E_s/(1-\nu_s)=1.8\times10^{11}$ Pa), t_s the thickness of the silicon wafer, and δ the deflection at the center of a surface scan over a distance D. In most cases D was 50 mm.

A. Results

The results of the measurements on 2 in. wafers for the ASM reactor are gathered in Table VI. The refractive index, the nonuniformity in the index, the stress, the deposition rate, and the thickness nonuniformity are graphically displayed as a function of the gas flow ratio R for two different levels of temperature and pressure in Figs. 3–7.

Some wafers were of such a low quality (i.e., their thickness was very nonuniform), that relatively large errors in the measured stresses occurred, and no meaningful data could be obtained. The σ_0 measurements for these cases have been omitted from Table VI. In order to obtain the desired response surfaces, these experiments have been repeated in another reactor (Tempress) with 3 in. wafers. The resulting data are shown in Table VII. Also, some other data obtained

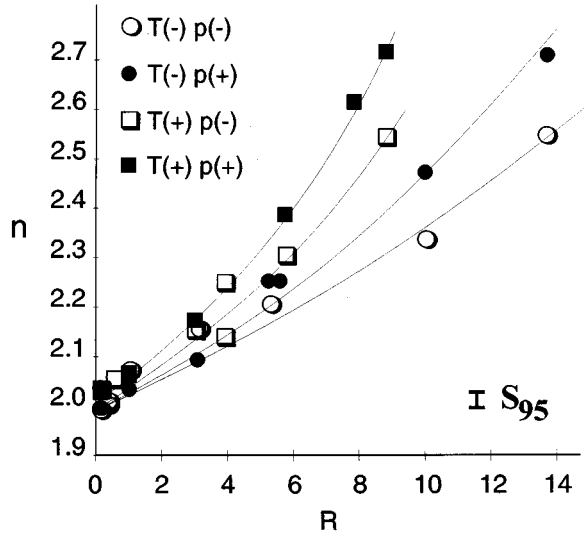

FIG. 3. Refractive index vs R for films deposited at $T(-)=800$ °C or $T(+)=850$ °C and at $p(-)=200$ mTorr or $p(+)=410$ mTorr. S_{95} denotes the 95% significance level for the parameter on the vertical axis (see Table IX). The lines are guides to the eye and do not represent a physical model.

in the latter reactor and results obtained in a home-built reactor[11] are included in this table. All the data in Table VII corresponding to the − and + levels of p and T of Table V have been included in Figs. 3–7.

As before, the significance levels for the experimental design can be derived from the center point runs. Using only the data of the NC and ND runs in Table VI, we obtain the values listed in Table VIII. It can easily be checked that the center point values fit into the trends in Figs. 3–7. Furthermore, the refractive index and stress data obtained for similar runs in another reactor (samples NC15 and ND4 in Table

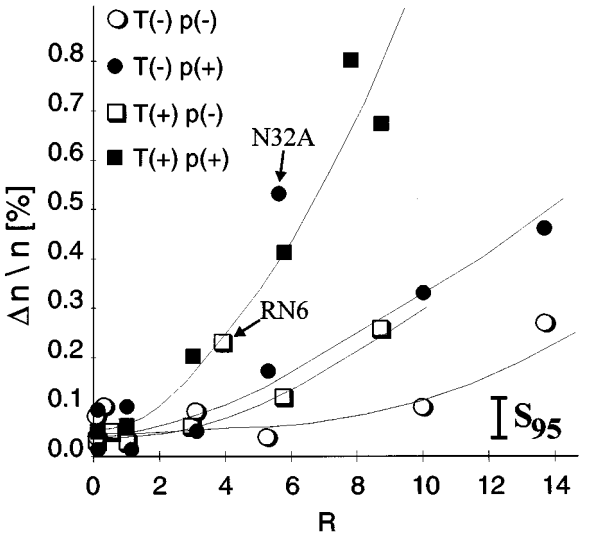

FIG. 4. Refractive index nonuniformity vs R for films deposited at $T(-)=800$ °C or $T(+)=850$ °C and at $p(-)=200$ mTorr or $p(+)=410$ mTorr. The arrows indicate data which do not agree with the general trends (see also remarks to Fig. 3 and the text).

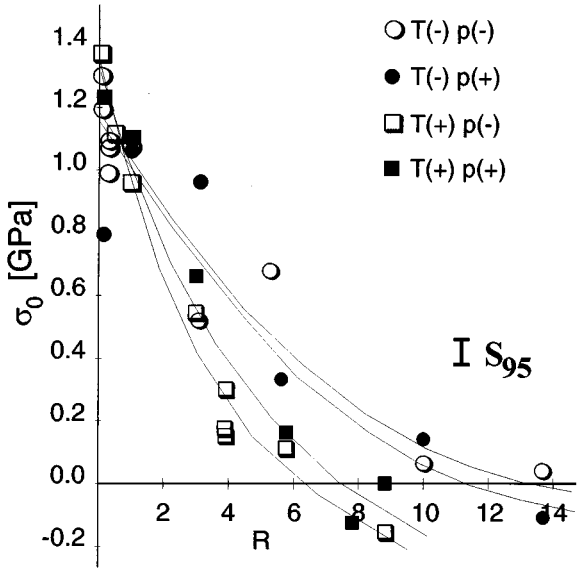

FIG. 5. Graphs illustrating the effects of the deposition parameters on the residual stress σ_0 (see also remarks to Fig. 3).

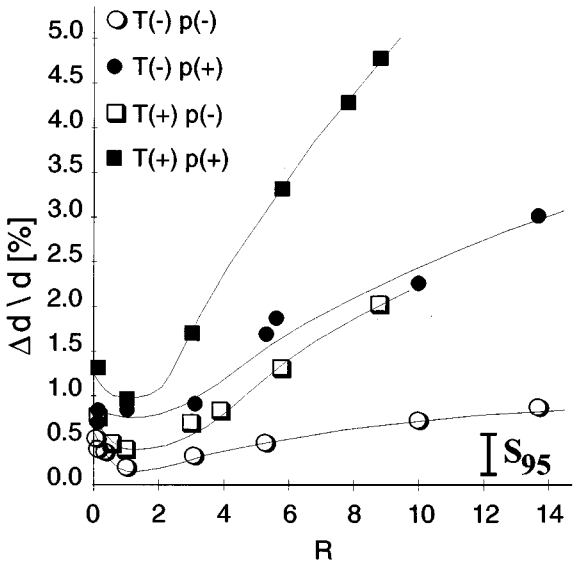

FIG. 7. Thickness nonuniformity vs R for films deposited at $T(-)=800$ °C or $T(+)=850$ °C and at $p(-)=200$ mTorr or $p(+)=410$ mTorr (see also remarks to Fig. 3).

VII) are in reasonable agreement with the data in Table VIII; however, some discrepancies exist in the deposition rate and thickness nonuniformity data for the center point runs in the two reactors (compare, e.g., NC15 with the mean values for the NC runs in Table VIII, see also the data points marked with arrows in Figs. 4 and 6).

B. FTIR and XRD

For samples RN5 and RN6 (Table VII) some FTIR measurements were performed, in order to obtain information about the hydrogen concentration in the Si_xN_y layers; for comparison a measurement on a plasma enhanced CVD (PECVD) Si_xN_y film was also included (see Ref. 14 for deposition conditions). For sample RN5 an absorption peak was found at 3280 cm^{-1}, which can be attributed to the N–H bond stretching mode.[20] The measured resonance frequency was rather low, compared to values of 3300–3335 cm^{-1} reported by others;[21–24] the shift to a lower frequency may be due to N–H–N hydrogen bonding.[23,25] For sample RN6 no IR absorption for the N–H stretching mode was found, while in the PECVD sample a rather intense absorption peak was found at 3310 cm^{-1}. In contrast to samples RN5 and RN6, where no Si–H stretching resonance was found, in the PECVD sample a peak was found at 2180 cm^{-1}; this frequency compares well with reported values for Si–H stretching in Si_xN_y, which range from 2160 to 2220 cm^{-1}.[21–24] All investigated samples contain a strong absorption band at ~860 cm^{-1}, which is attributed to asymmetric Si–N bond stretching;[20] between the different samples some minor differences in the shape and width of this band were observed, but these were not analyzed further.

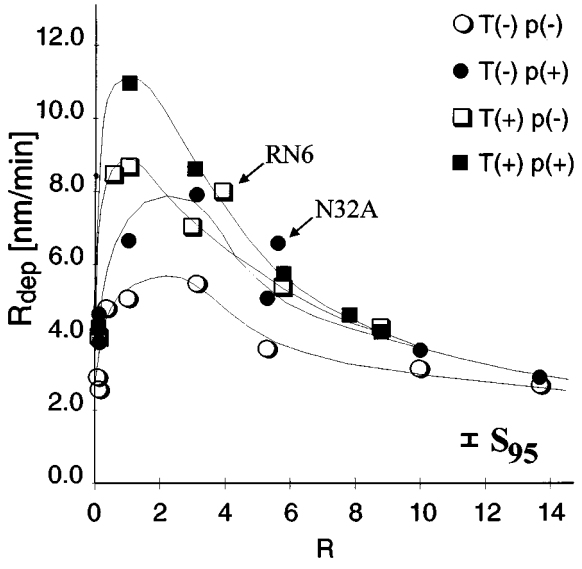

FIG. 6. Deposition rate in nm min^{-1} vs R for films deposited at $T(-)=800$ °C or $T(+)=850$ °C and at $p(-)=200$ mTorr or $p(+)=410$ mTorr. The arrows indicate data which do not agree with the general trends (see also remarks to Fig. 3 and the text).

From the absorption intensities of the Si–H and N–H stretching bands and reported absorption cross sections[26] we estimated the following hydrogen concentrations: for sample RN5: $(7\pm3)\times10^{21}$ cm^{-3}, with all hydrogen atoms bonded to nitrogen; for the PECVD sample: $(6\pm2)\times10^{21}$ cm^{-3} H atoms bonded to nitrogen and $(1.8\pm0.5)\times10^{21}$ cm^{-3} bonded to silicon; in sample RN6 no hydrogen was detected. These concentration data compare well with values reported by others.[4,27]

Several samples were studied by XRD, but no diffraction peaks other than those belonging to the Si substrate were found, indicating that the Si_xN_y films are amorphous; the Si crystallites mentioned in literature[28] were not observed.

TABLE VII. Additional data, obtained in different LPCVD reactors[a]

Wafer id.	Reactor	T	p	R	n	$\Delta n/n$ in %	σ_0 in MPa	R_{dep} in nm/min	$\Delta d/d$ in %	d in nm
N45	ASM	+	−	0.52	2.051	0.05	1110±40	8.45	0.46	92.9
N46	ASM	+	+	7.8	2.616	0.80	−130±80	4.58	4.29	82.5
N30A	Tempress	−	+	0.13	1.993	0.01	790±110	4.60	0.82	82.7
N32A	Tempress	−	+	5.6	2.252	0.53	330±140	6.56	1.86	105.0
N47	Tempress	−	−	3.1	2.154	0.09	520±170	5.47	0.33	120.3
N48	Tempress	−	+	3.1	2.091	0.05	960±110	7.86	0.90	78.6
NC15	Tempress	−	0	5.3	2.170	0.09	610±90	5.89	0.97	88.3
ND4	Tempress	+	0	5.3	2.321	0.30	⋯	7.60	0.86	106.4
RN5	Tempress	−	−	0.33	2.008	0.10	1090±40 1070±80[b]	4.77	0.37	439.1
RN6	Tempress	+	−	3.9	2.138	0.23	300±50 300±20[b]	8.0	0.83	404.8
X	Tempress	+	−	3.9	2.25	⋯	150±30 170±30[b]	⋯	⋯	1000
Y	Home-built	−	−	0.33	2.0	⋯	900[b]	⋯	⋯	370

[a]See also Table VI; all wafers are of size 3 in. except N45 and N46, which are 2 in.; for samples RN5, RN6, and X the wafer spacing was 9 mm; data for wafer X from Ref. 19, for sample Y from Ref. 11. All stress measurements by wafer curvature method, except the values marked with footnote b.
[b]Measured by the bulge method as described in Ref. 13. All other measurements were done in the same way as for the experiments in Table VI.

C. Statistical evaluation of phase II

Although it was not the main goal of the experimental design of phase II, the experiments of this phase in fact include a 2^3 factorial design similar to the one performed in phase I. Statistical evaluation of this 2^3 factorial will not only lead to a clear overview of the importance of the factors, which now also include temperature, but will also give valuable information about the reproducibility of the deposition experiments and the consistency of the experimental methods used (like the effect of the use of a different method for residual film stress measurement in phases I and II).

The factorial design we are referring to here consists of the samples with identification numbers N25, N28, N30, N33, N35, N39, N40, and N44 (see Table VI). Since it was established in a previous section that the residual film stress data of films deposited in different reactors are consistent, the σ_0 value obtained for sample N30A (Table VII) can be used to fill in the void for sample N30 in Table VI. The determination of the main and interaction effects of this design, containing the factors T and p (with the high and low levels as given in Table V), and gas flow ratio R (with lower level 1.00 and higher level either 8.78 or 10.0), is elaborated in Table IX, using Yates's algorithm.[6] Although the higher level of R is not the same for the complete design, relevant information can still be obtained.

It can be seen in Table IX that R has a significant effect on all responses, except the deposition rate. The latter is in clear contradiction with the results in Table IV, where R was found to be the most important factor for R_{dep}. The reason for this discrepancy can be seen in Fig. 6: the deposition rates at the low value of R (i.e., 0.1, for wafers N25, N30(A), N35, and N40) and at the high value of R (i.e., 10.0 for wafers N28 and N33, and 8.78 for wafers N39 and N44), are not very different, therefore we find only a small effect for R in Table IX. In the 2^3 factorial experiment leading to Table IV, however, the lower level for R was chosen at the value 1, which happens to be a gas flow ratio rather close to the maximum in the curve of growth rate versus R (see Fig. 6), so that here a large effect of R is found. This result shows one of the serious drawbacks of a factorial experiment with only two levels: if the levels are chosen on either side of a maximum in the response (as is the case in Table IX), too small effects may be found and misleading conclusions will be drawn.

The effect of temperature was not investigated in phase I. The results of phase II indicate that it has a significant influence on the refractive index and its nonuniformity, growth rate, and thickness nonuniformity. Its influence on residual stress is smaller than the 95% significance level. In view of the results of Sekimoto,[2] this small influence of temperature on the residual stress was unexpected and is in contradiction with the trends indicated in Fig. 5. The fact that the data in Table IX do not indicate temperature as an important factor for the stress is mainly caused by the different high levels for R (10.0 for $T=800$ °C and 8.78 for $T=850$ °C). These levels were chosen such that only a small apparent temperature effect is obtained (see Fig. 5). The two-factor interaction

TABLE VIII. Average values and standard deviations for calibration runs.

Parameter	n	$\Delta n/n$ in %	σ_0 (MPa)	R_{dep} (nm/min)	$\Delta d/d$ (%)
NC mean	2.210	0.106	660	3.91	1.23
NC S_1	0.008	0.006	50	0.18	0.06
ND mean	2.321	0.25	210	4.82	2.55
ND S_1	0.020	0.05	40	0.06	0.28
Mean of N25, N25A, N28, N30, N33	2.165	0.13	700	3.20	0.92
Mean of N35, N39, N40, N44	2.328	0.25	330	4.15	2.22

TABLE IX. Calculated effects for the implicit 2^3 factorial in phase II.[a]

Effect	n	$\Delta n/n$ in %	σ_0 (MPa)	R_{dep} (nm/min)	$\Delta d/d$ (%)
Mean	2.266	0.20	585	3.74	1.63
R	0.501	0.28	−1150	0.06	1.64
p	0.072	0.17	−90	0.42	1.27
T	0.125	0.11	50	0.83	1.18
pR	0.084	0.15	210	−0.23	0.88
RT	0.101	0.14	−230	−0.03	0.72
pT	0.013	0.04	100	−0.37	0.38
pRT	0.007	0.05	−60	0.09	0.23
S_1[a]	0.020	0.05	50	0.18	0.28
S_{95}[a]	0.032	0.08	80	0.29	0.45

[a]See also footnotes to Table IV. The significance level S_1 for each response was taken equal to the largest of the two S_1 values in Table VIII.

effects involving T, especially the one involving both T and R, are found to have an important influence on all responses (again with the exception of the small effect on the deposition rate of the interaction involving R). The interaction involving all three factors may be ignored for all of the responses.

The phase II results indicate that pressure variations have a large effect on n, $\Delta n/n$, R_{dep} and $\Delta d/d$, and a minor effect on σ_0. Similar results were obtained in the experiments of phase I. Concerning the effect of the interaction of p with R, the results in phase II are also similar to those of phase I, with the exception of the deposition rate, which shows a smaller response to the pR interaction effect, for the reasons discussed above.

With respect to curvature, it may be clear that in this case the center point runs cannot be compared directly with the mean values obtained in Table IX, because of the two different sets of center point levels which were used. The mean value of the NC runs should now be compared with the mean of runs N25(A), N28, N30, and N33 (i.e., the runs at $R=0.1$), while the mean values of the ND runs should be compared with the average of runs N35, N39, N40, and N44 (runs at $R=8.78$ or 10.0). These averages have been included in Table VIII. As discussed above, a significant deviation, i.e., curvature, is found for the growth rate versus R behavior.

The main goal of phase II was to obtain results useful for *response surface construction*.[6–8] The benefit of response surface construction is twofold: (i) it is the first step in the development of fundamental, physical–chemical models for the deposition process, and (ii) it indicates directions for further experimentation in order to optimize the deposition system for a specific application. Figures 3–7 are in fact projections in a specific plane of such response surfaces. Considering the levels which we have chosen for the experiments of phase II, a probably better way to graphically display the response surfaces would be to construct contour or surface plots (see, e.g., Ref. 29) for a specific response as a function of p and R, and to do so for two different values of T, viz., 800 and 850 °C. Since such an exercise does not provide any new information, but is merely a more convenient and perhaps more illustrative way to present the data, we have not constructed such plots.

Summarizing the results of phases I and II, we can say that we have found that (referring to Figs. 3–7, and taking into account the significance levels listed in Table IX) both an increase in pressure and temperature result in a significant increase in the refractive index. The rate at which the index changes as a function of the gas flow ratio becomes more rapid with increasing temperature or pressure. Both an increase in temperature and pressure result in a higher deposition rate. For large R values the thickness nonuniformity rises to unacceptably high values, especially at the higher temperature level and high pressures. The nonuniformity in the index is always below 0.7%. Similar to the observations made for the nonuniformity in the thickness, the nonuniformity in the index increases at high R values and when the temperature or pressure are raised. Concerning the residual stress in the films, we conclude that the main factor is the gas flow ratio R, that temperature also has a significant effect, and that pressure variations are not so important.

V. INTERPRETATION IN TERMS OF PHYSICAL–CHEMICAL MODELS

From a fundamental point of view it would be interesting to establish the physical (or chemical) laws which govern the behavior of the experimental system being studied. The data obtained in the experiments of phases I and II should-allow us to do so. In the following section we shall try to establish physically plausible models for the film properties studied in this work, using models from literature, where available.

A. Refractive index and its nonuniformity

Inspection of the literature shows that the two main parameters that determine the refractive index of Si_xN_y films are the Si/N ratio[5,30–33] and the atomic density.[33,34] Some authors[31,32,35] have also related the refractive index to the hydrogen content of the films, but this is probably only an indirect correlation, since the lower index which has been found for films with a high H content may be caused by the lower atomic density of these films.[32,34,36] The latter is the reason that PECVD Si_xN_y films deposited from SiH_4–NH_3 mixtures, which contain high amounts of hydrogen, systematically show lower refractive index values than the generally more dense LPCVD films.[27,34,35,37,38]

Generally it is found that the refractive index increases with the Si/N ratio.[5,22,39] According to Knolle[33] this is due to the large polarizability of Si with respect to that of N, so that with an increasing Si/N ratio the net polarizability will increase, leading to a higher value for the index n. In order to fit the refractive index data as a function of R, we have followed the following procedure: as a first approximation we calculated the Si/N ratio for each sample. This was done as follows: the data of Table IV indicate that the Si/N ratio is not significantly dependent on pressure or total gas flow. Although Table IV indicates nonzero curvature for the relation between the Si/N ratio in the film and R (as can be concluded from the fact that the mean of the center point runs is not equal to the mean value of the regular runs in Table IV), we assume as a first approximation that the Si/N

ratio is linearly dependent on the gas flow ratio R. Applying linear regression analysis[6] to the Si-*LVV*:N-*KLL*-ratio AES data in Table III, we find the following relation:

$$\mathrm{Si/N} = (0.73 \pm 0.02) + (0.032 \pm 0.007)R. \quad (3)$$

This relation suggests that the minimum attainable Si/N ratio is that of the stoichiometric composition Si_3N_4, so nitrogen-rich films will not be formed. The latter is consistent with reported experimental data on LPCVD deposition of silicon nitride from gas mixtures with NH_3/DCS ratios of up to 30.[4,5,40] It is also in agreement with the results of a thermodynamic analysis of the SiH_2Cl_2–NH_3 system,[41] which predicts that the excess NH_3 will not lead to incorporation into the solid, but will decompose to form the gases N_2 and HCl.

Subsequently we used Eq. (3) to calculate the Si/N ratio for each of the samples in Table VI, and first tried to fit the refractive index data with the aid of the method described by Knolle,[33] which is based on the so-called ''Bruggeman effective medium approximation.'' To do this, we assumed that the Si_xN_y films consist of random configurations of amorphous Si_3N_4 and Si phases. Unfortunately, an acceptable fit with the above method could only be obtained for a physically unrealistic n-value of 13.4 for the amorphous Si phase, and a (reasonable) value of 2.04 for the amorphous Si_3N_4 phase. Therefore we also used the model described in Refs. 5 and 21, in which it is assumed that the refractive index of the silicon-rich films is a ''bond-density-weighted linear combination'' of two reference refractive indices,[5] viz., those of amorphous silicon (a-Si) and amorphous stoichiometric silicon nitride (a-Si_3N_4). This model can be formulated as follows:

$$n = \frac{\{4(\mathrm{Si/N}) - 3\}n_\infty + 6n_{3/4}}{4(\mathrm{Si/N}) + 3} \quad (4)$$

with n_∞ the refractive index of a-Si and $n_{3/4}$ that of a-Si_3N_4. The contribution of small amounts of N–H bonds, which may be present in some of our films, was not taken into account here. A least-squares regression analysis of the data in Tables VI and VII with Eq. (3) gives the values shown in Table X. It can be seen that the fitting values for a-Si_3N_4 are acceptable (reported values are 1.98[5] and 1.953),[33] but those for a-Si are significantly higher than the value of 3.3 used for a-Si in Ref. 22, or the value of 3.86 of crystalline Si (Zhang *et al.*[16] used $n_\infty = 3.86$ and $n_{3/4} = 1.99$ to calculate Si/N from their measured n values). A close examination of the least-squares fits showed that the most likely reason for the discrepancies is that the assumption of a linear Si/N vs R relation, as formulated in Equation (3), is not correct. The procedure we followed next was: we used Eq. (4) to calculate the ''real'' Si/N value for each sample, with $n_\infty = 3.9$ and $n_{3/4} = 2.03$, and subsequently fitted the obtained Si/N vs R values with the quadratic equation

$$\mathrm{Si/N} = A + BR + CR^2. \quad (5)$$

Good fits were obtained, with correlation coefficients of more than 0.9. The fitting results for each $T-p$ combination are shown in Table X. It can be seen that for the conditions of low p and low T the relation between Si/N and R is almost linear; the quadratic term becomes more important at higher temperatures. Note that Table X confirms the result found in phase I (Table IV) that p has a small effect on Si/N.

TABLE X. Fitting values for refractive index vs Si/N and Si/N vs R data.

	$T(-)p(-)$	$T(-)p(+)$	$T(+)p(-)$	$T(+)p(+)$
$n_{3/4}$[a]	2.03±0.02	2.00±0.06	2.03±0.06	2.02±0.10
n_∞[a]	4.2±0.3	5.0±0.6	5.1±0.9	6.4±1.1
A[b]	0.727	0.706	0.732	0.727
B[b]	0.032	0.032	0.031	0.029
C[b]	0.000 64	0.0023	0.0038	0.0079

[a]Fitting parameter for Eq. (4).
[b]Fitting parameter for Eq. (5).

The refractive index nonuniformity (Fig. 4) can be interpreted as a nonuniformity of the Si/N ratio in the film. Most probably these Si/N fluctuations are due to the depletion of DCS during transport from the edge to the center of the wafer, leading to a higher Si/N ratio at the edge and thus a higher refractive index, in agreement with the observations. A similar depletion effect was found by Zhang *et al.*,[16] who observed a decrease in refractive index in the downstream direction of the reactor tube for LPCVD of Si-rich Si_xN_y, an effect which was found to be more severe for higher R values. An implication of this interpretation is that the wafer spacing during film deposition plays a role in determining the index nonuniformity. Examination of our experimental data shows that we find deviating nonuniformity data (see Fig. 4) for situations in which the wafer spacing during deposition was different from the majority of the experiments. However, the results are inconsistent: a higher nonuniformity is expected if the spacing is smaller, which is indeed the case for experiment N32A (spacing 4.5 instead of 6.6 mm); on the other hand, experiment RN6 also shows an unexpectedly high index nonuniformity, although it was performed with a larger wafer spacing (9 mm). It is also remarkable that in these particular two experiments the growth rate was inconsistently high, while the thickness nonuniformity was consistent with the general trends (see Fig. 7). We have no explanation for these peculiar results.

B. Deposition rate and thickness nonuniformity

In the literature a few theoretical models have been presented to describe the kinetics of silicon nitride deposition in LPCVD systems.[16,42–45] Experimentally, these models have only been tested thoroughly for the deposition of nearly stoichiometric Si_3N_4.[16,43,44] Peev *et al.*[42] discuss four different kinetic models for the deposition of silicon nitride:

(a) interaction between DCS and NH_3 takes place after adsorption on active surface sites of the same kind (Langmuir–Hinshelwood mechanism); adsorption is described by a Langmuir isotherm (i.e., the adsorption enthalpy on all surface sites is equal and independent of whether or not nearby sites are occupied);
(b) adsorption takes place according to a Freundlich iso-

therm (i.e., the adsorption enthalpy of species shows a logarithmic change with the partial pressure of the species);

(c) interaction between DCS and NH_3 takes place after adsorption on active surface sites of a different kind; adsorption is described by a Langmuir isotherm;

(d) interaction takes place between adsorbed NH_3 species and DCS gas molecules (Rideal–Ely mechanism); adsorption of NH_3 is described by a Langmuir isotherm (similarly, the reaction may take place between adsorbed DCS and NH_3 gas).

For each of these four models Peev *et al.*[42] have derived equations describing the relation between film deposition rate and NH_3 and DCS gas partial pressures. They conclude that model B best describes their experimental results for stoichiometric Si_3N_4 films. The following equation describes the deposition rate in nm/min as a function of the precursor partial pressures, according to this model B

$$R_{\mathrm{dep}} = k \frac{M}{\rho} p_{\mathrm{DCS}}^{b} p_{\mathrm{NH_3}}^{c}, \tag{6}$$

where k is a reaction contant (which includes adsorption parameters according to a Freundlich isotherm[42]), M and ρ are the molecular mass and the mass density of Si_3N_4, respectively, p_{DCS} and $p_{\mathrm{NH_3}}$ are the partial pressures of DCS and NH_3, respectively, and b and c are empirical numbers which, according to Ref. 42, have the values 0.49 and 0.46, respectively. The partial pressures are related to the ratio R used in our study as follows:

$$p_{\mathrm{DCS}} = \frac{pR}{R+1}, \quad p_{\mathrm{NH_3}} = \frac{p}{R+1} = p - p_{\mathrm{DCS}}. \tag{7}$$

We investigated whether the rate Eq. (6) fits our deposition rate data (Fig. 6). Figure 8 shows plots of the logarithm of R_{dep} versus the logarithm of the product of p_{DCS} and p_{NH3}. Such plots should result in straight lines, if the powers b and c in Eq. (6) are the same, and in fact this is the case for all our results; the corresponding fitting parameters are shown in Table XI. We also tried fits with different values of b and c, but these fits were not nearly as good as fits with equal b and c values.

Although it is not clear what an activation energy actually means if adsorption occurs via a Freundlich isotherm, it is in principle possible to use the offset fitting parameters in Table XI to calculate apparent activation energies for film deposition, with the aid of the following equation (which is derived from the familiar Arrhenin

$$\ln\left\{k_{T(+)}\frac{M}{\rho}\right\} - \ln\left\{k_{T(-)}\frac{M}{\rho}\right\} = \frac{-Eo,_{\mathrm{act}}}{\mathscr{R}}\left\{\frac{1}{T(+)} - \frac{1}{T(-)}\right\} \tag{8}$$

in which E_{act} is the activation energy and $\mathscr{R}$ the gas constant. The apparent activation energies which can be derived from the data in Table XI are: for $p(-)$:E_{act}=66 kJ/mol, and for $p(+)E_{\mathrm{act}}$=20 kJ/mol. It thus seems that the activation energy for the formation of Si-rich Si_xN_y is lower, than that of stoichiometric Si_3N_4, considering reported values of 151[9], 169.4[42] and 142–151[44] kJ/mol^{-1}. It might therefore be that an important factor determining the rate of the reactions in the silicon-rich regime is the diffusion of reactants or reaction products in the gas phase (which in general leads to low activation energies). However, more data are needed to clarify this.

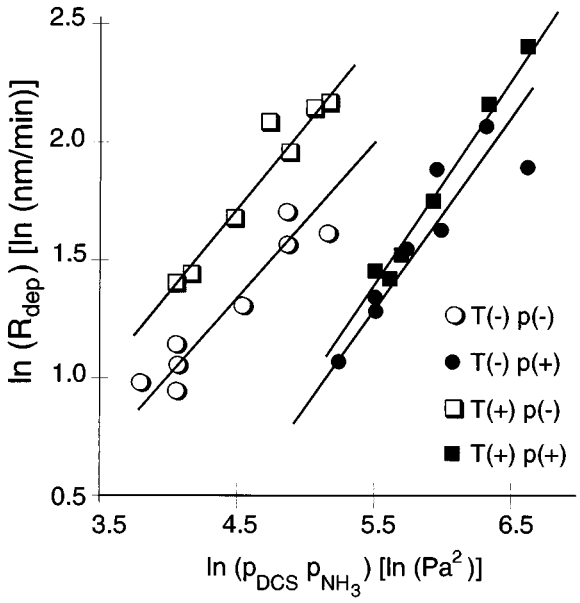

FIG. 8. Double-logarithmic plots of the deposition rate vs gas partial pressures (see the text).

There are two serious points we want to make about the model described above; these two aspects make us doubt whether the model is entirely correct. First, it has to be mentioned that we completely ignored the relations that exist between the factor M/ρ in Eq. (6) and the gas phase composition. This is, of course, not correct: it is expected that the molecular mass M is directly related to the Si/N ratio-in the film, and therefore depends on R in the gas phase. If Si/N were known [as we have discussed above, Si/N ratios in the film may be derived from the refractive index, see Eq. (4) and Table X], the molecular mass can easily be calculated. Data for the mass density of the films are less easy to estimate (see, e.g., Ref. 16). We tried to obtain these data by measuring the weight of the wafers before and after removal of the films, estimating the area of the films by dividing the mass of the silicon wafers without films by its mass density and the measured wafer thickness, and subsequently calculating the mass density of the films by dividing the measured film mass by this area and the measured thickness of the film. However, because of the rather low thickness of most of the films (around 100 nm, see Table VI) no accurate values for the mass density could be obtained.

A second point is the fact that for the $T(+)$ experiments the maximum in the deposition rate occurs for $R=1$ (see Fig. 6), which suggests that the rate Eq. (6) for these cases has a form in which indeed $b=c$; this can easily be checked by calculating the R value at which the maximum for R_{dep} in Eq. (6) should occur, which is: $R=b/c$. On the other hand,

the $T(-)$ experiments, in which the maximum seems to occur for $R=3$, suggest that for these cases b is not equal to c, but rather that $b=3c$, which is not consistent with the trends in Fig. 8. Inspection of Fig. 6 shows that the position of the maximum at $R=3$ is, however, only determined by one experimental point in each of the two curves for $T(-)$, viz, experiments N47 and N48 (see Table VII). If we leave out these two points, the maximum could well be located at $R=1$. It might be that these two experimental points, obtained in a different reactor than most of the other points, have been subject to some unknown experimental error (possibly a higher wafer spacing during deposition), and therefore do not fit into the general trends in Fig. 6 (although they fit in reasonably well in the trends in Figs. 3, 4, 5, and 7).

Thickness nonuniformity is generally explained by mass transport effects, leading to a higher deposition rate at the edge than in the center of a wafer, either because of a depletion of reactive species during transport from the edge of the wafer to the center, or because of the larger supply volume of reactive species at the edge of the wafer with respect to the center (a lower surface-to-volume ratio at the edge of the wafer). This explanation probably also holds for our experiments. It is observed that the mass transport effect is higher for higher R values, which is probably caused by a smaller diffusion length for the reactive silicon species (probably $SiCl_2$);[50] the concentration of this species will show a strong depletion from the edge to the center of the wafer, which not only gives a reduction in growth rate, but also a decrease in Si/N ratio in the film, and therefore a lower refractive index at the center (see also above). The fact that the deposition rate nonuniformity increases at higher pressures and at higher temperatures confirms the above: a higher pressure will decrease the diffusion length of the species, while a higher temperature leads to a higher concentration of reactive species, and therefore to an increased reaction probability of the species during its diffusion.

Our experiments were for the largest part performed on 2 in. wafers, with a few experiments on 3 in. silicon wafers. The question arises whether the results obtained here are also applicable to wafer sizes of 4 and 6 in. wafers, which are more common in a production environment. Comparison of our data for 2 and 3 in. wafers indicates that the results for these two sizes fit in the general trends, except for the uniformity data (Figs. 4 and 6). Generally the nonuniformity is higher for the larger wafer size, although one should also take into account the effect of wafer spacing. In our view these results can be extrapolated to still larger wafer sizes, with the same general trends. We expect that for these larger wafer sizes the nonuniformities, observed for larger R values, can be reduced by optimization of the wafer spacing (or the wafer boat configuration).

C. Residual stress

Our results show (see Fig. 5) that the parameters which control the residual stress in Si-rich Si_xN_y layers are, in decreasing order of importance, R, T, and p. These results are in very good quantitative agreement with those of Sekimoto *et al.*,[2] who have investigated the influence of R and T on residual stress and refractive index of the films, and also agree well with those of Refs. 46 and 47.

As to the origin of the residual stress, it is clear that the stress is not caused by a different thermal expansion between film and substrate, because this would lead to a tensile stress of only 10–15 MPa[48,49] for a deposition temperature of 800–850 °C. The stress is therefore of intrinsic origin. A plausible explanation for the intrinsic stress in silicon nitride films was offered by Noskov *et al.*,[35] who argue that the large tensile stress in stoichiometric Si_3N_4 results from the shrinkage of the bulk of the film during and after growth, caused by dissociation of Si–H and N–H bonds and rearrangement of the dangling bonds to stable Si–N bonds. Evidence for their model is found in the fact that the tensile stress in their films increases as a result of annealing, and probably also in the fact that the residual stress after annealing depends on the thickness of the film.

Considering the fact that we have found that the amount of hydrogen in Si-rich films deposited at a gas flow ratio R of 3.9 is below the IR measurement limit, combined with the considerable decrease in stress in these films with respect to stoichiometric films, the model of Noskov *et al.* seems to give a good qualitative explanation for the observed dependence of the residual stress on R.

VI. SUMMARY AND PERSPECTIVES FOR MICROMECHANICAL APPLICATIONS

In this article we have presented a systematic investigation of the influence of process parameters on the mechanical and optical properties of LPCVD Si_xN_y films, with the aid of a full factorial experimental design. The most relevant parameters determining the properties of the films, as well as the deposition rate and nonuniformities of properties across a wafer, were found to be, in decreasing order of importance, the gas flow ratio of Si and N containing species, the temperature, and the pressure during the deposition process. The relations between properties and deposition parameters were fitted with plausible physical–chemical models.

The established relations would allow us to optimize the LPCVD process for certain applications. This would require a final set of experiments; the specific application intended will determine the direction of experimentation. For instance, in the field of micromachining and micromechanical sensors and actuators, the major interest lies in locating a set of parameters leading to an as low as possible film stress. The data of Fig. 5 indicate that this would require high gas ratios R. For such conditions, however, the nonuniformity in deposited film thickness is fairly large, which would mean that in the specific application field of micromachined mechanical sensors like resonator sensors[1,11] an unacceptable nonuniformity in sensor sensitivity across a wafer would result. Furthermore, the fabrication of the free-standing beams, membranes, and cantilevers included in such devices requires long periods of exposure of the silicon nitride films to, e.g., aqueous KOH solutions; the etch rate of the films in such solutions is low, however it depends on the Si/N ratio in the

films.[11,14] Finally, because of the nonuniformity in thickness as well as in composition of the film (as evidenced by the refractive index nonuniformity) we also expect a nonuniformity in the residual stress across the wafer surface, which would lead to mechanical structures with unequal properties. Thus, optimization of the films for this particular application is complicated, and can probably only be tackled successfully in a not too long period of time with experimental designs. Our results indicate, e.g., that for micromechanical structures as described above conditions exist for which low-stress films can be deposited, without unacceptable increases in nonuniformity. These films have been used already in numerous micromechanical devices, like condenser microphones,[19,51] membranes with corrugations for stress relief,[52,53] flow sensors,[1,11,54] and resonant strain gauges.[1,11]

ACKNOWLEDGMENTS

The authors thank A. van de Berg (CMO, University of Twente) for AES, H. Tissing (AMOLF Amsterdam) for RBS, M. J. Anders (RIM, University of Nijmegen) for FTIR measurements, J. Taalman for wafer curvature measurements, G. Roelofs for RIE experiments, and M. de Boer for LPCVD experiments and ellipsometer measurements. H. A. C. Tilmans acknowledges the financial support of Johnson Controls Nederland B.V. and of the Dutch technology research foundation FOM-STW.

[1]S. Bouwstra, R. Legtenberg, H. A. C. Tilmans, and M. Elwenspoek, Sens. Actuators A **21–23**, 332 (1990).
[2]M. Sekimoto, H. Yoshihara, and T. Ohkubo, J. Vac. Sci. Technol. **21**, 1017 (1982).
[3]R. S. Rosler, Solid State Technol. **20**, April 1977, p. 63.
[4]P. Pan and W. Berry, J. Electrochem. Soc. **132**, 3001 (1985).
[5]T. Makino, J. Electrochem. Soc. **130**, 450 (1983).
[6]G. E. P. Box, W. G. Hunter, and J. S. Hunter, *Statistics for Experimenters* (Wiley, New York, 1978).
[7]O. Kempthorne, *The Design and Analysis of Experiments* (Wiley, New York, 1952).
[8]W. G. Cochran and G. M. Cox, *Experimental Designs*, 2nd ed. (Wiley, New York, 1957).
[9]J. A. Gregory, D. J. Young, R. W. Mountain, and C. L. Doherty, Jr., Thin Solid Films **206**, 11 (1991).
[10]J. Wilson and G. DePinto, J. IES July/August 1991, p. 26.
[11]S. Bouwstra, Ph.D. thesis, University of Twente, 1990.
[12]K. E. Crowe and R. L. Smith, J. Electrochem. Soc. **136**, 1566 (1989).
[13]E. I. Bromley, J. N. Randall, D. C. Flanders, and R. W. Mountain, J. Vac. Sci. Technol. B **1**, 1364 (1983).
[14]J. G. E. Gardeniers and N. G. Laursen, Sens. Materials **5**, 189 (1994).
[15]E. G. Keim and K. Aite, Fresenius Z. Anal. Chem. **333**, 319 (1984).
[16]S.-L. Zhang, J.-T. Wang, W. Kaplan, and M. Östling, Thin Solid Films **213**, 182 (1992).
[17]G. G. Stoney, Proc. R. Soc. London Ser. A **82**, 172 (1909).
[18]A. Brenner and S. Senderoff, J. Res. Natl. Bur. Stand. **42**, 105 (1949).
[19]P. R. Scheeper, Ph.D. thesis, University of Twente, 1993.
[20]D. V. Tsu, G. Lucovsky, and M. J. Mantini, Phys. Rev. B **33**, 7069 (1986).
[21]H. J. Stein and H. A. R. Wegener, J. Electrochem. Soc. **124**, 908 (1977).
[22]E. Bustaret, M. Bensouda, M. C. Habrard, J. C. Bruyère, S. Poulin, and S. C. Gujrathi, Phys. Rev. B **38**, 8171 (1988).
[23]Z. Yin and F. W. Smith, Phys. Rev. B **42**, 3666 (1990).
[24]B. Reynes, C. Ance, J. P. Stoquert, and J. C. Bruyère, Thin Solid Films **203**, 87 (1991).
[25]M. Maeda and H. Nakamura, J. Appl. Phys. **58**, 484 (1985).
[26]V. I. Belyi, L. L. Vasilyeva, A. S. Ginovker, V. A. Gritsenko, S. M. Repinsky, S. P. Sinitsa, T. P. Smirnova, and F. L. Edelman, *Silicon Nitride in Electronics, Materials Sci. Monographs 34* (Elsevier, Amsterdam, 1988) p. 90.
[27]G. N. Parsons, J. H. Souk, and J. Batey, J. Appl. Phys. **70**, 1553 (1991).
[28]E. A. Irene, N. J. Chou, D. W. Dong, and E. Tierney, J. Electrochem. Soc. **127**, 2518 (1980).
[29]R. Legtenberg, H. V. Jansen, M. J. de Boer, and M. Elwenspoek, J. Electrochem. Soc. **142**, 2020 (1995).
[30]K. E. Bean, P. S. Gleim, R. L. Yeakley, and W. R. Runyan, J. Electrochem. Soc. **114**, 733 (1967).
[31]G. M. Samuelson and K. M. Mar, J. Electrochem. Soc. **129**, 1773 (1982).
[32]W. A. P. Claassen, W. G. J. N. Valkenburg, F. H. P. M. Habraken, and Y. Tamminga, J. Electrochem. Soc. **130**, 2419 (1983).
[33]W. R. Knolle, Thin Solid Films **168**, 123 (1989).
[34]H. Dun, P. Pan, F. R. White, and R. W. Douse, J. Electrochem. Soc. **128**, 1555 (1981).
[35]A. G. Noskov, E. B. Gorokhov, G. A. Sokolova, E. M. Trukhanov, and S. I. Stenin, Thin Solid Films **162**, 129 (1988).
[36]J. C. Bruyère, C. Savall, B. Reynes, M. Brunel, and L. Ortega, J. Phys. D **26**, 713 (1993).
[37]V. S. Nguyen, N. S. Burton, and P. Pan, J. Electrochem. Soc. **131**, 2348 (1984).
[38]S. V. Nguyen, J. Electron. Mater. **16**, 275 (1987).
[39]J. Gyulai, O. Meyer, J. W. Mayer, and V. Rodriguez, Appl. Phys. Lett. **16**, 232 (1970).
[40]S. Hasegawa, Y. Amano, T. Inokuma, and Y. Kurata, J. Appl. Phys. **72**, 5676 (1992).
[41]K. Spear and M. Wang, Solid State Technol. **20**, April 1977, p. 63.
[42]G. Peev, L. Zambov, and Y. Yanakiev, Thin Solid Films **189**, 275 (1990).
[43]C. E. Morosanu, D. Iosif, and E. Segal, Thin Solid Films **92**, 333 (1982).
[44]K. F. Roenigk and K. F. Jensen, J. Electrochem. Soc. **134**, 1777 (1987).
[45]T. Sorita, T. Satake, H. Adachi, T. Ogata, and K. Kobayashi, J. Electrochem. Soc. **141**, 3505 (1994).
[46]O. Tabata, K. Kawahata, S. Sugiyama, and I. Igarashi, Sens. Actuators **20**, 135 (1989).
[47]R. A. Stewart, J. Kim, E. S. Kim, R. M. White, and R. S. Muller, Sens. Materials **2**, 285 (1991).
[48]A. K. Sinha, H. J. Levinstein, and T. E. Smith, J. Appl. Phys. **49**, 2423 (1978).
[49]J. A. Taylor, J. Vac. Sci. Technol. A **9**, 2464 (1991).
[50]J. G. E. Gardeniers and L. J. Giling, J. Cryst. Growth **115**, 542 (1991).
[51]P. Scheeper, W. Olthuis, and P. Bergveld, J. Microelectromech. Syst. **3**, 36 (1994).
[52]V. L. Spiering, S. Bouwstra, J. F. Burger, and M. Elwenspoek, J. Micromech. Microeng. **3**, 243 (1993).
[53]M. W. Hamberg, C. Neagu, J. G. E. Gardeniers, D. J. Ijntema, and M. Elwenspoek, Proc. IEEE Workshop Micro Electro Mech. Syst., Amsterdam, Jan. 29–Feb. 2, 1995, p. 106.
[54]T. S. J. Lammerink, N. Tas, M. Elwenspoek, and J. H. J. Fluitman, Sens. Actuators A **37–38**, 45 (1993).